ACS APPLIED MATERIALS & INTERFACES

Research Article

www.acsami.org

Direct Imaging of Mechanical and Chemical Gradients Across the Thickness of Graded Organosilicone Microwave PECVD Coatings

Colin J. Hall,*[,†] Peter J. Murphy,[‡] and Hans J. Griesser[‡]

[†]Ian Wark Research Institute and [‡]Mawson Institute, University of South Australia, Mawson Lakes 5095, Australia

Supporting Information

ABSTRACT: The characterization of variations in the chemical composition and ensuing mechanical properties across the thickness of coatings with continuously varying compositions through their thickness (graded coatings) presents considerable challenges for current analytical techniques in materials science. We report here the direct imaging of nanomechanical and chemical gradients across cross-sections of an organosilicone coating fabricated via microwave plasma enhanced chemical vapor deposition (PECVD). Cross-sectional nanoindentation was used to determine the mechanical properties of uniform and graded organosilicone coatings. Both hardness and modulus across the coatings were directly measured. Additionally, "modulus mapping" on cross-sections was used to map the complex modulus. For the graded coating, it was found that variations in the complex modulus was predominantly due to varying storage modulus. It was observed that at the interface with the substrate there was a low storage modulus, which linearly increased to a relatively high storage modulus at the surface. It is proposed that the increase in stiffness, from the substrate interface to the outer surface, is due to the increasing content of a cross-linked O−Si−O network. This mechanical gradient has been linked to a change in the Si:O ratio via direct compositional mapping using ToF-SIMS. Direct mapping of the mechanical and compositional gradients across these protective coatings provides insight into the changes in properties with depth and supports optimization of the critical mechanical performance of PECVD graded coatings.

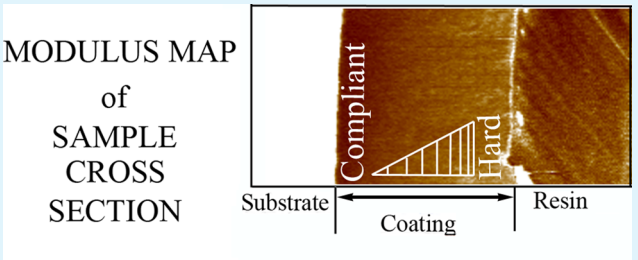

KEYWORDS: *nanoindentation, graded, thin films, plasma-enhanced chemical vapor deposition (PECVD), mechanical properties, plastic*

1. INTRODUCTION

Protective thin film coatings are of considerable interest for the purpose of protecting substrate "bulk" materials against abrasion, scratching, corrosion, and other damage. For plastic materials in particular, such coatings can open up many new applications. Protective coatings on plastics, and in particular hardcoatings, have been used successfully in a variety of applications such as in ophthalmic lenses,[1,2] automotive headlights,[3] and aircraft windows.[4] These hardcoatings are commonly deposited as a liquid and then cured by thermal or UV radiation to form an abrasion resistant and durable surface treatment. An alternative technique is the deposition of a protective coating via vacuum deposition. One vacuum technique of considerable interest and practical utility is microwave plasma-enhanced chemical vapor deposition (PECVD), which offers fast deposition rates and the ability to grade chemically and mechanically through the thickness of the coating.[5,6]

Currently used hardcoatings are uniform in composition; however, often it may be preferable to utilize coatings whose chemical composition varies continuously across their thickness from the substrate interface to the outer surface. The compositional variation in such "graded" coatings can be used to tailor the ensuing mechanical properties; for example, a protective coating on polycarbonate should possess mechanical properties similar to those of the substrate at that interface, whereas the outer surface of the coating should be much harder so as to be more abrasion resistant.

It is, however, challenging to characterize graded coatings across their thickness, both chemically and mechanically. The mechanical characterization of thin films has been a focus of research for many years.[7,8] The development of nanoindentation techniques has led to an increase in research and micromechanical understanding of thin film systems.[9−12] As this measurement technique has evolved, improvements have allowed smaller and shallower penetrations to be made. This has resulted in the mechanical properties of thin layers to be determined independent of the influence of the substrate. Following simple rules, one can obtain reliable results for single homogeneous layers for both hardness and modulus.[10] This information can then be used to engineer coatings for a particular application. Nonhomogenous (graded or multilayer) coatings, in contrast, represent a more complex scenario in terms of mechanical characterization. While indicative proper-

Received: November 15, 2013
Accepted: January 3, 2014
Published: January 3, 2014

ties can be measured on single layers deposited under different conditions, extrapolating single layer properties to a continuously graded layer may lead to errors in interpretation.[13] Depth sensing indentation normal to the surface can also lead to errors in data analysis. As a result there has been considerable work on directly measuring the properties of graded coatings. Li and Bhushan[14] have shown a variation in contact stiffness due to a change in mechanical properties with depth for magnetic tapes; however, the values determined were influenced by the underlying layers. Similar limitations were also noted by Poornesh et al.[15] on the mechanical properties of graded catalyst layers. It is well-established that indentation normal to the surface suffers from sublayer influences and, as such, cannot reliably determine inhomogeneous film properties.[16−18] In an attempt to overcome such issues, Linss et al.[19] have shown a level of success by utilizing multiple spherical indents using indenter tips of different radii. However, the most promising results have been demonstrated using cross-sectioning, and then direct mechanical indentation.[6,16,20−22]

Direct indentation of cross-sectioned samples has been conducted mostly on multilayer systems.[16,17,20] and to a lesser extent on graded materials.[20,23] To help improve the resolution of the measurements, some researchers have employed small-angle cross-sectional (SACS) nanoindentation.[16,17,24] However, even at small angles there is considerable influence on individual measurements by the surrounding sample volume and, additionally, sample cross-sectioning and preparation can influence the results. These limitations have hampered the wider application of this technique in the coating engineering field.

The study reported here-in addresses limitations of cross-sectional analysis, by utilizing nanoindentation with increased resolution and reducing the change per unit volume occurring within the grading during measurements. First, nanoindentation equipment with very high resolution was employed in this study. Second, for the coating system under study, it was possible to deposit layers with significant thickness, of ∼10 μm. At this thickness the rate of change in mechanical properties across the coating was small enough to be within the resolution of the nanoindentation systems used. This coating thickness was afforded by the high deposition rates of our microwave PECVD process. Deposition rates of up to ∼40 nm/s were achieved, allowing 10 μm films to be deposited without significant substrate heating or deviation from "real world conditions", where typically a coating thickness of 3−8 μm is used as a protective hardcoating. This range of thicknesses is challenging to achieve with more conventionally powered radio frequency (rf) PECVD systems and, as such, there is limited information in the literature on the direct mechanical and chemical mapping of these types of coatings.[16]

This study has applied high-resolution nanoindentation to directly measure the nanomechanical properties across a continuously graded coating. Hardness and modulus values for a homogeneous and a graded coating were determined and the results compared. Additionally, dynamic indentation was used to perform modulus mapping to determine the complex modulus across cross sections and determine both storage and loss modulus values with submicrometer resolution. For correlation with mechanical characterisations, analysis of the compositional gradient achieved during deposition was performed by ToF-SIMS. The relative performance in two critical tests (adhesion and abrasion) was determined on the homogeneous and graded coating and compared to a commercially available liquid applied homogeneous hardcoating.

Such characterisations of graded coatings support work toward designed protective coatings particularly for the protection of plastic substrates, such as poly(methyl methacrylate) (PMMA) and polycarbonate (PC), for example, for automotive lights and mirrors, acrylic windows, and ophthalmic lenses.

2. EXPERIMENTAL SECTION

A. Deposition and Sample Preparation. Substrates of polycarbonate, aluminum foil, and microscope glass slides were cleaned with methanol in an ultrasonic bath for 5 min and then blow-dried with dry nitrogen before loading into the vacuum chamber. Deposition was performed in a custom-built reactor as shown in Figure 1. The design is based on systems developed by both Leybold

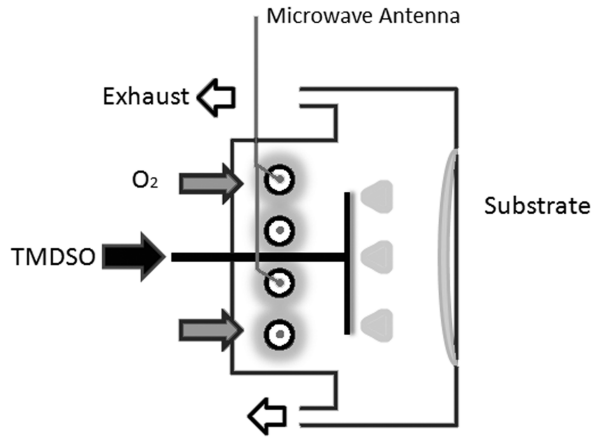

Figure 1. Schematic diagram of the microwave PECVD chamber.

Optics GmbH and Muegge GmbH.[25,26] and used more recently by Neykova et al.[27] Microwave power up to 6 kW and at a frequency of 2.45 GHz was fed into both ends of 4 copper antennas. The antennas were fed down the center of four aluminum oxide tubes. The tubes are located along one wall of the chamber and are semienclosed to form the plasma zone which feeds directly into this region. The total volume of the plasma glow is ∼9700 cm^3 and requires the plasma power levels used in this study to produce uniform glow zones. The monomer vapor, to enable deposition, was fed separately through a gas ring aimed directly at the substrates which are located facing the tubes. Monomer and gas flows were regulated via mass flow controllers (MFC) calibrated for the specific gases used. The chamber was evacuated with a Roots blower (605 m^3/h EH500, Edwards) and Rotary pump (80 m^3/h, E2M80, Edwards) combination. The chamber pressure was monitored with a capacitance manometer (10 Torr, model #628, MKS) and the system was controlled via a Programmable Logic Controller (PLC).

The deposition of organosilicone coatings was achieved using a mixed vapor phase consisting of the monomer tetramethyldisiloxane (TMDSO) (Sigma-Aldrich, Australia) and oxygen (ultrahigh purity). The flow of TMDSO was kept constant at 100 sccm (standard cubic centimeters per minute) for all coatings. Homogeneous coatings for performance testing and nanoindentation normal to the surface were deposited on PC at oxygen flows of 200 and 500 sccm to a thickness of ∼4 μm. Graded coatings for performance testing of ∼4 μm thickness were deposited on PC with oxygen linearly ramped from 200 to 500 sccm. Coatings for cross-sectional analysis of ∼10 μm thickness were produced with either a constant oxygen flow of 500 sccm for 240 s or a linearly ramped flow from 200 to 500 over 290 s. The pressure during deposition varied from 40 to 70 Pa as a result of the oxygen ramp. Samples were stored in laboratory conditions at 22 °C and RH

between 30% and 60% in between sample preparation and measurements.

Samples of 1 × 1 cm^2 size were embedded and cut normal to the surface in an epoxy based mounting resin (Epofix, Struers), see the Supporting Information, Figure S1. Cross-sectioning was carried out with a Minitom diamond cutoff machine (Struers) to reveal a suitable section of the coating. The samples were polished with a Tegramin 30 system (Struers), using 500 and 1000 grit SiC paper with water for 1 min each and then polished with decreasing particle size diamond polish (DP −Suspension A; 9, 3, 1, and 0.25 μm) with nonaqueous lubricant for 5 min each. The samples were cleaned with an ethanol rinse followed by Milli-Q water and then blown dry with dry nitrogen gas stream.

A commercially available hardcoating (PHC587B, Momentive Performance Materials, Germany) was used as a reference in the performance testing. This siloxane based hardcoating was deposited and cured as per the manufacturers specifications to a thickness of ∼3 μm on PC substrate.

B. Characterization. Indentation measurements were performed with two different indentation systems, namely a UMIS 2000 (CSIRO) and a TI-950 TriboIndenter (Hysitron). Nanoindentation was carried out using a UMIS2000 (CSIRO, Australia) with a Berkovich tip following ISO14577.[21] Normal indentation was performed to a maximum load of 1 mN and unloaded to 20% of maximum load with a 20 μm spacing. Cross-sectional nanoindentation was performed under the following conditions. Three sets of 20 indents to a maximum load of 0.35 mN and unloaded to 20% of maximum load were performed at 2 μm intervals across the sample surface. For all nanoindentation analysis, corrections were made for initial penetration, machine compliance (0.00015 μm/mN) and area correction factor (previously determined from indents on fused silica). Hardness and modulus were calculated following the Oliver and Phar method[28] and then averaged to give a final value.

Additional nanoindentation was carried out with a TI-950 TriboIndenter nanomechanical test instrument (Hysitron, Minneapolis, MN, USA). A diamond cube-corner indenter probe was used. Three lines of 14 indents were performed perpendicular to the film interface on each sample to obtain hardness and modulus across the coating surface. The spacing between indents was 1 μm. Each indent consisted of a 5 s loading segment to a peak load of 0.2 mN, a 5 s hold segment, and a 5 s unloading segment. A 15 × 15 μm^2 scan was performed across the surface of each sample using the dynamic modulus mapping technique. The interpretation of the references to color in the modulus mapping figures is contained in the web version of this article. The same diamond cube-corner probe was utilized. The measurement was performed at 200 Hz with a set-point of 4.0 μN and a dynamic load of 0.5 μN. The dynamic load was selected to produce displacement amplitudes of approximately 1−2 nm within the film.

Time of flight−secondary ion mass spectrometry (ToF-SIMS) experiments were performed using a Physical Electronics Inc. PHI TRIFT V nanoTOF instrument (Physical Electronics Inc., Chanhassen, MN, USA) equipped with a pulsed liquid metal $^{79+}$Au primary ion gun (LMIG), operating at 30 kV energy. Dual charge neutralization was provided by an electron flood gun and 10 eV Ar^+ ions. Measurements were performed at a pressure of $\lesssim 5 \times 10^{-6}$ Pa. "Bunched" Au_1 instrumental settings were used to optimize mass resolution. Prior to analyses, the surface was sputter cleaned for 10 s using a 20 kV C^{60} ion gun (Ionoptika, Southampton, UK). Spectra were collected in positive and negative SIMS modes, using a 25 by 25 μm raster area. ToF-SIMS spectra were calibrated using the WinCadenceN software (Physical Electronics Inc.). Particular care was required in the preparation of the coating for ToF-SIMS analysis. The coating was deposited onto an aluminum substrate and then embedded in silver loaded resin. The high conductivity of the mounting system avoided charge buildup during analysis. Data were collected from at least two positions per sample, to ensure that the overall data were representative of the samples. Three line scans per position per sample were generated across each cross-section. Each point on the line scan is an average of 7 pixels, which was equivalent to the width of the line.

Adhesion was measured according to ASTM D3359−02 in three different locations on three different samples. A quantitative measure of the level of adhesion is achieved by assessing the amount of coating removed from the cross-hatch area with adhesive tape, 3 M #600 (pull of force on metal 44 N/100 mm width).[29] This was then converted into a score from 0 to 5 using the standard rating system, where 0 indicates complete delamination and 5 indicating no coating has been removed

The abrasion resistance was determined by the Bayer abrasion test.[30] In this test a Taber oscillating abrasion tester (model 6100) was used as per previously described procedure.[31] In this test, the abrasion resistance is quantified by the Bayer ratio, which takes account of the change in haze of the sample before/after abrasion with reference to the haze change observed for a reference sample. Both the sample and the reference were measured for haze using a HunterLab UltraScan Pro instrument. In this study, an uncoated PC was used as the reference sample, for determination of the Bayer ratio. Thus, a Bayer ratio of 1 corresponds to the abrasion resistance of uncoated PC. The larger the determined Bayer ratio, the greater the abrasion resistance relative to the reference sample. Three samples per variant were tested and the results averaged.

3. RESULTS

A. Nanomechanical Analysis. Preliminary mechanical analysis was carried out with the UMIS system, normal to the surface, on the materials used in this study, that is, glass, PC, PMMA, mounting resin and two homogeneous coatings, see Table 1. The homogeneous coatings were deposited onto PC at a low oxygen flow to create a "compliant" layer and at high oxygen flow to create a "hard" layer. Deposition parameters were chosen to replicate conditions used to previously deposit protective coatings on polymer substrates.[32,33]

Table 1. Hardness and Modulus of Relevant Materials and Homogenous Coatings Deposited at Low and High Oxygen Flows[a]

material	sample	hardness (GPa)	modulus (GPa)
glass	substrate	6.9 ± 0.7	66.8 ± 8
resin	encapsulate	0.4 ± 0.05	5.2 ± 0.6
PC	substrate	0.2 ± 0.05	2.2 ± 0.5
PMMA	substrate	0.3 ± 0.05	3.5 ± 0.5
"compliant" homogenous coating On PC substrate	oxygen flow 200 sccm	0.2 ± 0.05	2.5 ± 0.3
"hard" homogenous coating On PC substrate	oxygen flow 500 sccm	1.2 ± 0.1	8.6 ± 0.8

[a]Measurements were performed using the UMIS nanoindenter, normal to the surface. Errors were determined from standard deviation of the measurements (n = 20).

Coatings of graded composition were deposited onto glass substrates for the purpose of cross-sectional analysis. A glass substrate was chosen so that a distinct difference in mechanical properties between the substrate, the coating, and the mounting resin could be observed. Normally these coatings would be deposited on a PC or PMMA substrate. As these coatings are designed to match the mechanical properties of these substrates, it was found with this arrangement, that it was difficult to identify the substrate−coating interface.

Figure 2 shows indentation data from the UMIS system with a graded coating. Cross-sectional analysis was carried out on the same indentation system as was used to determine the mechanical properties normal to the surface, data in Table 1. This allowed the direct comparison between the nanoindentation performed normal to the surface and that

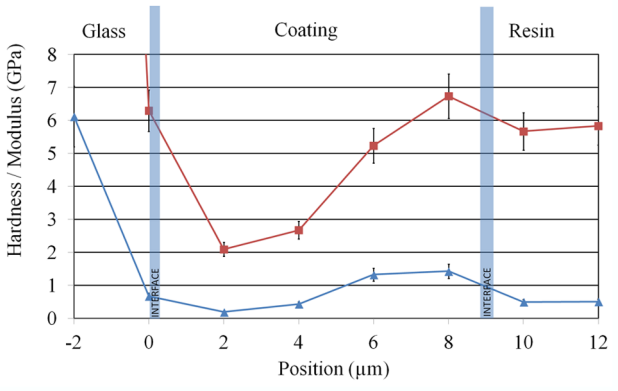

Figure 2. Mechanical properties of the graded coating as a function of position, as measured with the UMIS nanoindenter: hardness (▲) and elastic modulus (■). Error bars were determined from the standard deviation of 3 data sets. Shaded lines are located at the glass-coating-resin interfaces.

performed on the cross-section, using the same indentation protocol.

Indentation was only possible every 2 μm because of system limitations. The indent at position 0 μm has clearly been influenced by the interface with the glass, as the hardness and modulus values are higher at 0.7 and 6.3 GPa, respectively. At position −4 μm, the mechanical properties match those of glass, see Figure S2a in the Supporting Information. Note that the indents positioned at the 10 and 12 μm mark show decreased hardness and modulus values, because of the influence of the mounting resin. These points indicate the position of the substrate-coating and coating−resin interfaces. Four data points (positions 2 to 8) fall within the coating, and these data show a significant increase in both hardness and modulus. The low oxygen flow (soft) coating is representative of the conditions at the start of the grading and the high oxygen flow (hard) coating is representative of the conditions at the end of the grading. There is general agreement between values from indentations normal to the surface on homogeneous coatings to those recorded with cross-sectional indentation on a graded coating at the respective positions.

Further mechanical analysis was performed with a Hysitron TriboIndenter. This analysis directly compared a coating deposited under constant oxygen flow of 500 sccm (referred to as the uniform coating) with a coating deposited with increasing oxygen flow from 200 to 500 sccm (the graded coating). Figure 3a shows hardness and modulus values for the uniform coating at 1 μm intervals. It is noted that the measurements at the interface transition points of glass to coating (position −1 and 0 μm) and coating to resin (position 11 μm) show values between those of the glass and the coating at the first interface, and between coating and resin at the second interface. For these points, the mechanical properties were influenced by a combination of the materials at the interface and, as such, there was a volume averaging effect. At position −2 μm the mechanical properties match those of glass, see Figure S2b, c in the Supporting Information.

The size of the measurement transition was estimated from observation of the position at which the measurement returned to its "true" value. From the observations, it was estimated that each measurement point was influenced by the surrounding material out to a radius of ∼1 μm. The uniform coating has a hardness of ∼0.75 GPa and a modulus of ∼3.5 GPa. The data

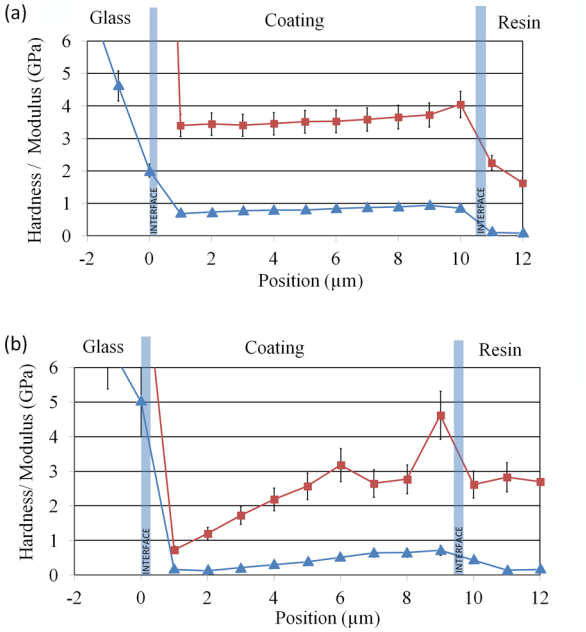

Figure 3. Mechanical properties as a function of position across the cross-section as measured by the Hysitron system: (a) for a uniform coating and (b) for a graded coating. Hardness (▲), and elastic modulus (■). Error bars were determined from the standard deviation of the 3 data sets. Shaded lines are located at the glass-coating-resin interfaces.

show that there was no significant change in mechanical properties across the cross-section, as would be expected from a uniform coating.

Figure 3b shows the nanomechanical data for the graded coating. At the interface with the substrate (glass) the coating has a hardness and elastic modulus of 0.16 and 0.83 GPa respectively. The mechanical properties of this layer are comparatively soft and flexible, as expected for a low oxygen flow organosilicone plasma coating.[34] A clear increase was observed across the cross-section with both the hardness and the modulus values at the coating-resin interface reaching 0.72 and 4.5 GPa respectively. The hardness and modulus values at this "outer" surface of the coating are comparable to those of the uniform coating deposited under the same conditions.

Both the UMIS and Hysitron data indicate a grading in the mechanical properties that is linear. A linear fit of the hardness and modulus data returns an $R^2 > 0.85$. It is noted that there is a difference in the absolute values between the two systems with the UMIS data tending to be higher in both hardness and modulus. This discrepancy most probably arises from a combination of different loads used in the indentation procedure (UMIS ∼0.35 mN and Hysitron ∼0.2 mN) and the use of differently shaped indenter tips. The Hysitron system used a cube corner indenter, whereas the UMIS system used a Berkovich tip, and the relative sharpness of the two tips would produce different sized plastic zones, which most likely accounts for the difference in results.[35]

B. Complex Modulus. Dynamic indentation was performed with the modulus mapping technique of the Hysitron TriboIndenter. A 15 × 15 μm^2 area was scanned with a low load to produce a high resolution map of the elastic properties of uniform and graded samples, specifically its complex modulus. At shallow indentation depths the indenter tip can be considered spherical;[10] and thus the response of the system

to the measurement was assumed to be purely elastic. The complex modulus can be separated into its real and imaginary parts, which are known as the storage and loss modulus, respectively. Figure 4 shows complex modulus, storage modulus and loss modulus maps for both uniform and graded coatings. In each image the glass substrate is on the left-hand side, the coating in the middle and the mounting resin on the right-hand side, arrows indicate each materials extent. There are some anomalies at the coating-resin interface, which are attributed to the small change in height at this interface produced during sample preparation. The change in modulus is depicted by a color change, as described by the scale bar at the bottom of the images. In all images a dark color corresponds to a low modulus and a light color corresponds to a high modulus. With this color scale, the glass substrate appears as completely white. Figure 4a shows a uniform color indicating a uniform modulus. Figure 4d shows a dark color at the substrate-coating interface changing to a lighter color at the coating-resin interface, as expected on the basis of the coating becoming harder with increasing oxygen flow across the cross-section.

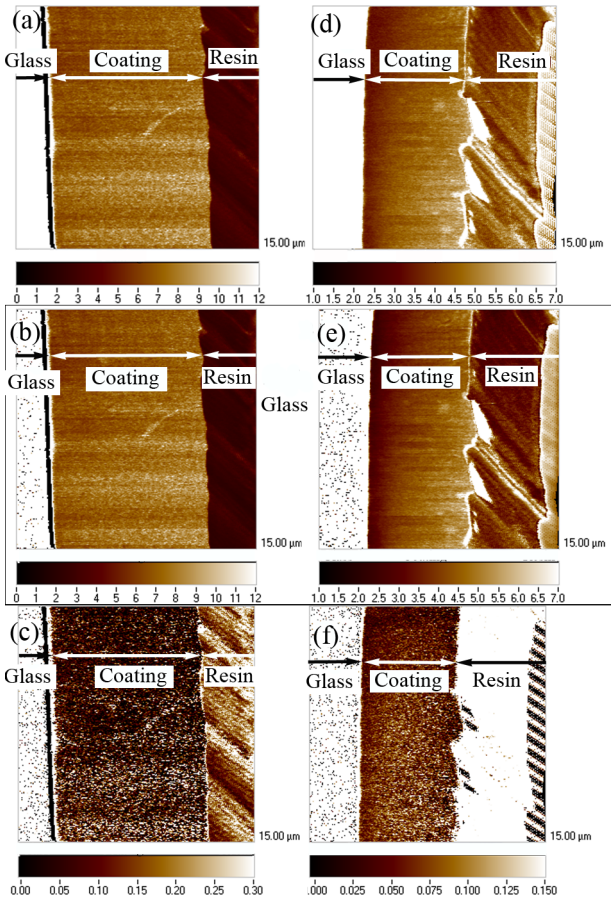

Figure 4. Modulus mapping imaging on samples produced with uniform oxygen flow showing (a) complex, (b) storage, and (c) loss modulus and graded oxygen flow showing (d) complex, (e) storage, and (f) loss modulus. Images are of a 15 × 15 μm square. Color bar indicates the magnitude of the modulus in GPa. Low modulus is indicated by a dark color, a high modulus by a light color.

The map image for the storage modulus for the uniform coating is shown in Figure 4b and for the graded coating in Figure 4e. The storage modulus for the uniform coating is homogeneous throughout the cross-section examined, as indicated by a constant color across Figure 4b. In contrast Figure 4e. shows a clear change in color from dark to light, indicating an increase in the storage modulus for the graded coating.

Figure 4c shows the mapping of the loss modulus of the uniform coating and Figure 4f for the graded coating. The loss modulus map shows some noise in the form of a grainy image, this is due to the small value of the loss modulus for these coatings, between 0 and 0.3 GPa. In Figure 4c, there is no change in color across the cross-section, indicating a uniform loss modulus. In Figure 4f, there is a slight dark region at the glass-coating region becoming lighter toward the interface between the glass substrate and the coating. This indicates a very small grading in the loss modulus for the graded coating.

Thus, in summary, the variation in oxygen flow during deposition to produce the graded coating has predominately resulted in a gradient of the storage modulus of the coatings, with only a small gradient observed in the loss modulus.

C. Chemical Analysis. Positive and negative ion scans were carried out by ToF-SIMS, and clear signals for Si^+, O^-, and Al^+ were detected. Despite precautions against charge build up, significant signals could not be detected for carbon-containing ions. It was expected that the carbon content of coatings would change with oxygen flow, as has been reported previously.[36] The intensity of Si^+ did not show any grading for either the uniform coating or the graded coating, in accord with expectations, as a previous study using XPS reported that the silicon content of a plasma coating is not influenced by the oxygen to TMDSO ratio.[36] Figure 5a shows the O^- signal from Tof-SIMS surface scans for the graded coating. A change in color, from dark to light, was observed in the cross-section, indicating an increase in the O^- signal from the substrate to the surface of the coating. The chemical map for the uniform coating showed a constant O^- signal across the cross-section (data not shown). Figure 5b shows an overlay image of the Si^+ and Al^+ signals, this more clearly defines the boundaries of the coating.

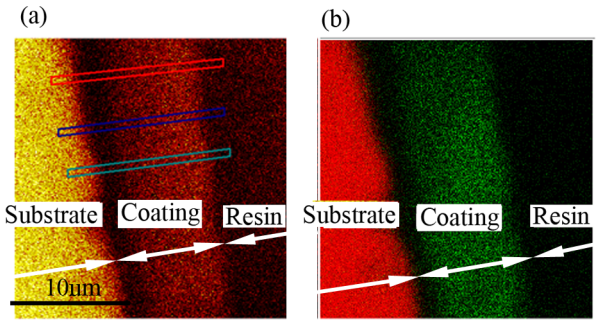

Figure 5. ToF-SIMS mapping of the graded coating (a) O^- (yellow) signal and (b) an overlayer of the Si^+ (green) and Al^+ (red) signal. Rectangular windows represent areas where the line scans where taken. Scale bar is 10 μm. Arrows indicate each materials extent.

Three line scans, as indicated by the colored rectangles in Figure 5a, were averaged and the average plotted in Figure 6. The substrate−coating interface has been defined as the midpoint between the substrates chemical signature and the coatings chemical signature. The interface has been nominally located at 0 μm position. The O^- signal measured at the substrate is high and this is most likely due to the presence of an oxide layer on the aluminum. The O^- signal drops significantly at the interface, indicating the beginning of the

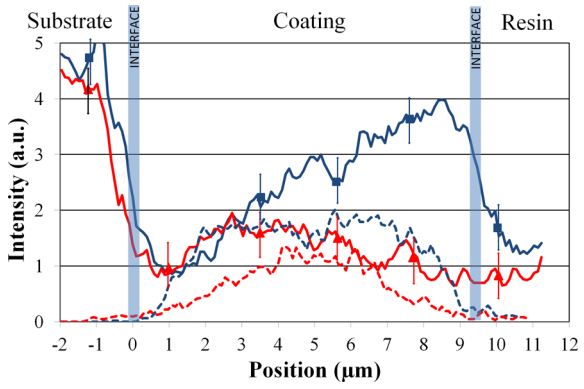

Figure 6. Line scans of the O^- (solid line) and Si^+ (dashed line) signal, which are an average of the three areas indicated by the rectangular windows for the uniform (red, ▲) and graded (blue, ■) samples. Error bars are indicative of the standard deviation between the three line scans performed on each sample. Shaded lines are located at the substrate−coating−resin interfaces.

low oxygen flow coating and rises again to a maximum at the resin interface. A clear increase in the O^- signal can be observed across the thickness of the graded coating and this increase matches the increase seen in mechanical properties.

D. Performance Testing. For automotive or aerospace applications, protective coatings on plastics must adhere well and provide an increased level of abrasion resistance. To establish the relative performance of homogeneous and graded coatings, we undertook performance-based testing. Homogenous and graded coatings were deposited on PC, their performance was assessed via adhesion and abrasion resistance, Table 2. The results show that the graded coating achieves a compromise between adhesion and abrasion resistance that homogeneous coatings cannot. It shows better adhesion and almost the same level of abrasion resistance to that of the "hard" coating. A commercial hardcoating was tested as a suitable performance reference.

Table 2. Performance Data Comparing Homogenous and Graded Coatings[a]

deposition conditions	oxygen flow (sccm)	adhesion (rating out of 5)	abrasion resistance (Bayer abrasion ratio)
"compliant" homogeneous coating	200	4 ± 0.5	2.2 ± 0.4
"hard" homogeneous coating	500	2 ± 0.5	5.1 ± 0.6
graded coating	200−500	4 ± 0.5	4.6 ± 0.7
PHC587B resin hardcoating	n.a.	5 ± 0.5	6 ± 0.9

[a]Errors were determined from standard deviation.

4. DISCUSSION

A. General Interpretation. Cross-sectional analysis has been successfully used to detect and image changes in mechanical and chemical properties between uniform and graded coatings. The measurements established that a linear increase in mechanical and chemical properties was achieved across the thickness of the graded coating. Previous work has predominantly used separate measurements at constant deposition parameters to measure the coatings characteristics. The characteristics of subsequent graded coatings made under continuously changing deposition parameters were then inferred from these previous measurements.[37,38] This technique can deliver good results that show a match between homogeneous coating properties and that of gradient coatings. It is postulated that this technique may miss important effects caused by continuous deposition. It also may not be feasible to produce individual coatings from a particular deposition system, or that these individual measurements are not representative of the continuous deposition.[39] Alternatively, direct indentation normal to the surface of graded materials has been conducted,[40] but suffers from discrepancies due to errors in the assumptions made and limitations in the modeling.[13]

This study has shown that the mechanical properties measured via normal indentation on separate coatings deposited under conditions representative of the start and finish of the grading (Table 1) agree with the start and end points of the cross-sectioned sample. As discussed above, one could infer the grading from these individual measurements; however, using direct indentation of the cross-section this study has identified that the gradient between these two points is indeed linear in nature. The data in Table 1 were closely compared with the indentation data in Figure 3. A slight discrepancy was observed in that the high oxygen flow coating displayed a higher modulus than the graded coating at the final point; this is most likely due to insufficient spatial resolution causing an averaging effect at the interface with the resin. This observation places a limitation on how to interpret the cross-sectioned indentation data at the interface, with either substrate or resin, highlighting that one must exercise caution when analyzing such regions.

Ideally, the concept of grading is such that a coating is made mechanically compliant at the interface with a polymer substrate and then the mechanical properties are increased so that, at the surface, the coating is hard and abrasion resistant. The compliant substrate interface addresses the problem of coating delamination by interfacial stress caused by flexing, temperature changes, and other effects. By matching the mechanical properties of the initial stages of the coating to that of the substrate, compatibility is enhanced and interfacial stresses are reduced. This concept has been discussed by Ramalingam and Zheng,[41,42] who studied high hardness coatings on metals, and Jen et al.,[43] who studied barrier films on Teflon. They both discuss the use of interlayers to achieve a mechanical match between substrate and coating. In the worked described here, we have transferred this concept to low temperature coatings on plastics using a graded coating to achieve the desired match in mechanical properties. Table 1 lists the hardness and modulus values of the two plastics that these coatings have been applied onto (PMMA and PC). The mechanical properties of the graded coating in the initial stages of the grading are ~0.2 and 2.1 GPa. The graded coating examined has achieved a close match in properties to those of both polymers (see Figure S3 in the Supporting Information for schematic).

On increasing the mechanical strength of the surface of the coating, a hard outer layer results in the imparting of abrasion resistance. The analysis presented in this study has confirmed that this concept has been achieved with these coatings. Preliminary performance in adhesion and abrasion resistance (Table 2) has shown that grading has led to an enhanced adhesion while abrasion resistance was maintained. A

comparison with the performance of a commercially available liquid resin hardcoating has shown that the graded coating requires further optimization. Further, mechanical and durability testing of such graded coatings will be reported elsewhere.

Potential errors due to long-range effects in the indentation measurements should be considered when interpreting these results. As can be seen in the transition between substrate and coating there was a 1−2 μm area in which the results are determined by a combination of the materials in the measured volume. This is in agreement with the results of Cedaka et al.;[44] however, this is no different to indentations performed at normal incidence or at small angles. These other techniques also suffer from unwanted influences from surrounding materials. Importantly, surface roughness effects should also be considered. There are two points to be made. First, both the uniform and graded coatings have been cross-sectioned and polished at the same time, and it was found that there was no significant difference in surface roughness between the two samples. As such, any surface roughness influence should be comparable for the two systems measured. Second, for the standard hardness and modulus measurements, penetration depths (h_p) were between 150 and 500 nm. The surface roughness was well below the suggested limit of $h_p/20$.[45] For dynamic indentation with a 4 μN indentation load, the penetration depth was approximately 15−20 nm. At these low penetration depths, the surface roughness was less than the 0.75 nm limit, and so would have had a minimal effect on the projected contact area.

The deposition rate has been shown to be influenced by the variation in the oxygen to monomer ratio.[36,46] At the beginning of the grading (TMDSO/O_2 = 100/200) the deposition rate was ∼27 nm/s, and this reached a maximum of ∼42 nm/s at TMDSO/O_2 = 100/360, after which it dropped slightly to ∼40 nm/s at TMDSO/O_2 = 100/500. Theoretically, this will result in the early part of the grading having a smaller thickness than the final part. Figure 7 shows the thickness calculated from the expected deposition rate, as the graded coating was deposited. A straight line, which represents the thickness that would result from a constant deposition rate, is also plotted for reference. Here the variations in deposition rate with oxygen content were small enough for the deviation from a straight line to be acceptable. The resolution of the mechanical and chemical measurements was not sufficient to reveal this deviation.

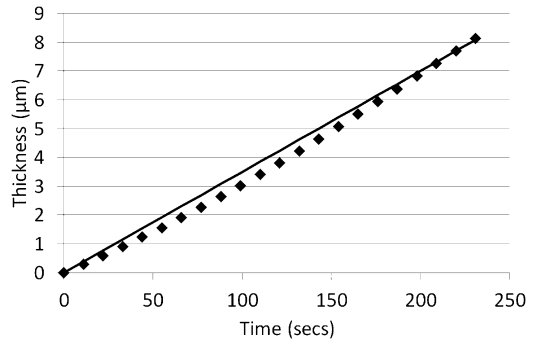

Figure 7. Calculated total thickness based on expected deposition rates at the various TMDSO and oxygen flows (♦) and solid black line representing the calculated thickness for a constant deposition rate.

B. Complex Modulus Interpretation. Complex modulus is a measure of the resistance of a material to deformation. It consists of two components, the real (storage modulus) and imaginary (loss modulus) parts. The storage modulus relates to a material's elastic response, and the loss modulus relates to a material's viscous response. At the measurement frequency used (200 Hz), the coating system studied had a high storage modulus and a small loss modulus; thus they can be described as viscoelastic. However, as the loss modulus is small, the material is deforming predominantly in an elastic manner. For the graded coating the change in mechanical properties across its thickness was observed to occur predominantly in the storage modulus component, that is, the observed grading resulted in changes of the elastic properties. At the substrate, the coating was compliant, which is desirable for use on plastic substrates, as this will give an enhanced mechanical match between substrate and coating. Such a result is advantageous for robust adhesion[47] and, as discussed earlier, is expected to enhance durability in performance based testing. The storage modulus linearly increased with thickness and at its surface the coating was stiff and is predicted to provide a high level of abrasion resistance. Previous work supports the validity of the approaches we have used to characterize our gradient coatings. Similar measurements were used to probe nanometer sized features by Shilo et al.[48] and were shown to produce superior resolution compared to other modulus mapping studies.[49]

The increase in storage modulus toward the surface corresponds with decrease in the TMDSO to oxygen ratio during deposition. Correspondingly, there is a change in the Si:O ratio in the coating as confirmed by the ToF-SIMS measurements. It has been reported[46,50−52] that oxygen gas added to a siloxane plasma performs a major role in the fragmentation process. The efficiency with which it changes the mechanical and chemical properties of a PECVD coating makes it a useful parameter for tuning coating properties. With the increase in oxygen flow into the chamber, an associated increase in pressure was observed. This would also act to reduce the mean free path of the gases and the increase the plasma density. Hegemann et al.[53,54] report on the previous work performed in this area, for large changes in pressure, a plasma can transition from a volume-dominated discharge to a corner-dominated discharge. However, in most cases, a limited pressure change has little to no effect on deposition rate and limited effect on film formation. In studies where pressure has been kept constant while the TMSDO to oxygen ratio varied, similar changes to coating chemistry and structure were reported.[50,51] As such, although the effect of the two parameters cannot be separated for this study, it is proposed that the oxygen driven reactions dominate the film formation.

Previous NMR and FTIR[55,56] studies have shown that coatings produced with high oxygen flow have a highly cross-linked O−Si−O network. Predominantly their network consists of Si−O in a Q (quaternary) structure, where Si is bound to 4 oxygen atoms. Coatings produced at lower oxygen flow tend to have more termination type bonds, O−Si−R where R can be H, OH, or CH_x. In NMR terms, the structure is made up of more M (monofunctional), D (difunctional), T (trifunctional) structures. This structural information can now be linked to the coating's increasing storage modulus, as described here. As the oxygen flow was increased the coating changed from a compliant low modulus coating to a stiff, high modulus and highly cross-linked structure. It appears reasonable to postulate that this increase in cross-linking is predominantly responsible for the increase observed in the storage modulus toward the surface of the graded coating.

This study has shown the feasibility of using nanomechanical mapping on cross sections of graded coatings to determine key mechanical and compositional characteristics. Further work is being undertaken to change the profile of the grading and to relate this to mechanical performance based analysis. It is intended to use the present cross-sectional analysis approaches to assist the optimization of graded coatings.

5. CONCLUSIONS

Cross-sectional mapping has been achieved for both mechanical and compositional properties of PECVD coatings. These techniques are essential tools for studies aiming to tailor such properties for better compliance with those of plastic substrates, such as polycarbonate. The mechanical cross-sectional data show that our organosilicone graded coatings indeed possessed the intended structure of a compliant substrate interface and a hard, abrasion resistant surface. Performance testing showed the enhanced adhesion and abrasion resistance of the graded coating over the homogeneous coating. The resolution of the hardness and modulus measurements was limited to 1 μm due to the influence of the surrounding material. However, the high deposition rates obtained with the microwave PECVD system has allowed sufficiently thick coatings to be deposited and characterized with acceptable resolution.

Modulus mapping using very low, oscillatory loads has provided high resolution 2D maps of homogeneous and graded coatings. It was found that the dominant change in the coating's complex modulus was in the storage modulus component. This has been associated with an increase in the O−Si−O network of the coating as the oxygen flow is increased. Complementary information was obtained via ToF-SIMS, which showed a linear change in the O^- ion signal across the graded coating. As such, the change in mechanical properties could be directly linked to a change in chemical composition. It is expected that such direct cross-sectional analyses will be useful for optimization of the profile in mechanical properties of graded coating so as to enhance durability performance.

■ ASSOCIATED CONTENT

Supporting Information

Schematics that show the sample mounted in cross-section and the mechanical matching achieved between substrates and graded coating; cross-sectional nanoindentation data that spans a wider scan length. This material is available free of charge via the Internet at http://pubs.acs.org.

■ AUTHOR INFORMATION

Corresponding Author

*E-mail: colin.hall@unisa.edu.au. Ph. +61 8 8302 3833. Fax +61 8 8302 5639.

Author Contributions

The manuscript was written through contributions of all authors. All authors have given approval to the final version of the manuscript.

Notes

The authors declare no competing financial interest.

■ ACKNOWLEDGMENTS

The authors acknowledge John Denman for conducting ToF-SIMS measurements, Ryan Stromberg of Hysitron for nanomechanical measurement and analysis, and Rick Fabretto for helpful comments. This research was supported by the Commonwealth of Australia through the Automotive Australia Cooperative Research Centre.

■ REFERENCES

(1) Samson, F. *Surf. Coat. Technol.* **1996**, *81*, 79−86.
(2) Caro, J.; Cuadrado, N.; González, I.; Casellas, D.; Prado, J. M.; Vilajoana, A.; Artús, P.; Peris, S.; Carrilero, A.; Dürsteler, J. C. *Surf. Coat. Technol.* **2011**, *205*, 5040−5052.
(3) Seubert, C.; Nietering, K.; Nichols, M.; Wykoff, R.; Bollin, S. *Coatings* **2012**, *2*, 221−234.
(4) Oguri, K.; Sekigawa, T. Aircraft window of synthetic resin having hard coated film and a method for producing the same. U.S. Patent 6 756 126, June 29, 2004.
(5) Beckmann, R.; Nauenburg, K. D.; Naumann, T.; Patz, U.; Ickes, G.; Hagedorn, H.; Snyder, J., A new high-rate deposition process for scratch- and wipe-resistant coatings for optical and decorative plastic parts. *Proceedings of the 44th Annual Technical Conference of SVC*; Philadelphia, PA, April 21−26, 2001 ; Society of Vacuum Coaters: Abuquerque, NM, 2001.
(6) Kaiser, M.; Baumgärtner, K. M.; Mattheus, A. Microwave based plasma technology. In *Proceedings of the 20th International Conference on Applied Electromagnetics and Communications*; Dubrovnik, Croatia, Sept 20−23 ; IEEE: Piscataway, NJ, 2010.
(7) Page, T. F.; Hainsworth, S. V. *Surf. Coat. Technol.* **1993**, *61*, 201−208.
(8) Han, S. M.; Saha, R.; Nix, W. D. *Acta Mater.* **2006**, *54*, 1571−1581.
(9) Fischer-Cripps, A. C. In *Nanoindentation*, 2nd ed.; Ling, F. F., Ed.; Mechanical Engineering Series; Springer: New York, 2004.
(10) Fischer-Cripps, A. C. *Surf. Coat. Technol.* **2006**, *200*, 4153−4165.
(11) Bhushan, B.; Li, X. *Int. Mater. Rev.* **2003**, *48*, 125−164.
(12) Gouldstone, A.; Chollacoop, N.; Dao, M.; Li, J.; Minor, A. M.; Shen, Y. L. *Acta Mater.* **2007**, *55*, 4015−4039.
(13) Fischer-Cripps, A. C. *Surf. Coat. Technol.* **2003**, *168*, 136−141.
(14) Li, X.; Bhushan, B. *Thin Solid Films* **2000**, *377*−*378*, 401−406.
(15) Poornesh, K. K.; Cho, C. D.; Lee, G. B.; Tak, Y. S. *J. Power Sources* **2010**, *195*, 2709−2717.
(16) Holzapfel, C. Nanoindentation mapping of physical properties. In *Proceedings of the Annual Holm Conference on Electrical Contacts*; Vancouver, BC, Canada, Sept 14−16, 2009 ; IEEE: Piscataway, NJ, 2009.
(17) Cech, V.; Trivedi, R.; Skoda, D. *Plasma Process. Polym.* **2011**, *8*, 1107−1115.
(18) Čekada, M.; Panjan, P. *Vacuum* **2001**, *61*, 235−240.
(19) Linss, V.; Schwarzer, N.; Chudoba, T.; Karniychuk, M.; Richter, F. *Surf. Coat. Technol.* **2005**, *195*, 287.
(20) Botero, C. A.; Jimenez-Piqué, E.; Kulkarni, T.; Fargas, G.; Sarin, V. K.; Llanes, L. *Surf. Coat. Technol.* **2011**, *206*, 1927−1931.
(21) Molina-Aldareguia, J. M.; Ocana, I.; Gonzalez, D.; Elizalde, M. R.; Sanchez, J. M.; Martinez-Esnaola, J. M.; Sevillano, J. G.; Scherban, T.; Pantuso, D.; Sun, B.; Xu, G.; Miner, B.; He, J.; Maiz, J. *AIP Conf. Proc.* **2006**, *817*, 104−109.
(22) Forster, A. M.; Michaels, C. A.; Sung, L.; Lucas, J. *ACS Appl. Mater. Interfaces* **2009**, *1*, 597−603.
(23) Steen, T. L.; Basu, S. N.; Sarin, V. K.; Murray, T. W. *AIP Conf. Proc.* **2007**, *894*, 217−224.
(24) Ziebert, C.; Ulrich, S. *J. Vac. Sci. Technol., A* **2006**, *24*, 554−583.
(25) Liehr, M., Device for producing plasma. U.S. Patent 6 194 835, May 27, 2001.
(26) Eberhard, R.; Eberhard, F.; Muegge, H., Device for generating plasma in vacuum container. D.E. Patent 19628954, Jan 22, 1998.
(27) Neykova, N.; Kozak, H.; Ledinsky, M.; Kromka, A. *Vacuum* **2012**, *86*, 603−607.
(28) Oliver, W. C.; Pharr, G. M. *J. Mater. Res.* **1992**, *7*, 1564−1580.
(29) *3M Datasheet: Scotch Transparent Film Tape 600, Report 70-0710-0229-2*; 3M: St. Paul, MN, 2003.

(30) *ASTM F735-6: Standard Test Method for Abrasion Resistance of Transparent Plastics and Coatings, Using the Oscillating Sand Method*; ASTM: West Conshohocken, PA, 2006.
(31) Evans, D.; Zuber, K.; Hall, C.; Griesser, H. J.; Murphy, P. *Surf. Coat. Technol.* **2011**, *206*, 312−317.
(32) Hall, C. J.; Murphy, P. J.; Griesser, H. J. *Plasma Process. Polym.* **2012**, *9*, 398−405.
(33) Hall, C. J.; Murphy, P. J.; Griesser, H. J. *Plasma Process. Polym.* **2012**, *9*, 855−865.
(34) Hegemann, D.; Vohrer, U.; Oehr, C.; Riedel, R. *Surf. Coat. Technol.* **1999**, *116−119*, 1033−1036.
(35) Woodcock, C. L.; Bahr, D. F. *Scr. Mater.* **2000**, *43*, 783−788.
(36) Griesser, H.; Murphy, P.; Hall, C. Craze resistant plastic article and method of production. U.S. Patent 20080096014 A1, April 24, 2008.
(37) Gu, Y.; Nakamura, T.; Prchlik, L.; Sampath, S.; Wallace, J. *Mater. Sci. Eng., A* **2003**, *345*, 223−233.
(38) Tompkins, B. D.; Fisher, E. R. *Plasma Process. Polym.* **2013**, *10*, 779−791.
(39) Ziebert, C.; Bauer, C.; Stüber, M.; Ulrich, S.; Holleck, H. *Thin Solid Films* **2005**, *482*, 63−68.
(40) Suresh, S.; Giannakopoulos, A. E.; Alcala, J. *Acta Mater.* **1997**, *45*, 1307−1321.
(41) Ramalingam, S.; Zheng, L. *Tribol. Int.* **1995**, *28*, 145−161.
(42) Zheng, L.; Ramalingam, S. *Surf. Coat. Technol.* **1996**, *81*, 52−71.
(43) Jen, S.-H.; George, S. M.; McLean, R. S.; Carcia, P. F. *ACS Appl. Mater. Interfaces* **2012**, *5*, 1165−1173.
(44) Čekada, M.; Panjan, M.; Panjan, P.; Kek-Merl, D. *Surf. Coat. Technol.* **2006**, *200*, 6554−6557.
(45) *ISO14577-1:2002 Metallic material—Instrumented indentation test for hardness and materials parameters*; International Organization for Standardization: Geneva, Switzerland, 2002.
(46) Bapin, E.; von Rohr, P. R. *Surf. Coat. Technol.* **2001**, *142−144*, 649−654.
(47) Huang, C.; Yu, Q. *J. Appl. Polym. Sci.* **2010**, *116*, 245−251.
(48) Shilo, D.; Drezner, H.; Dorogoy, A. *Phys. Rev. Lett.* **2008**, *100*, 035505.
(49) Tromas, C.; Stinville, J. C.; Templier, C.; Villechaise, P. *Acta Mater.* **2012**, *60*, 1965−1973.
(50) Goujon, M.; Belmonte, T.; Henrion, G. *Surf. Coat. Technol.* **2004**, *188−189*, 756−761.
(51) Patelli, A.; Vezzù, S.; Zottarel, L.; Menin, E.; Sada, C.; Martucci, A.; Costacurta, S. *Plasma Process. Polym.* **2009**, *6*, S665−S670.
(52) Saloum, S.; Naddaf, M.; Alkhaled, B. *Vacuum* **2008**, *82*, 742−747.
(53) Hegemann, D.; Brunner, H.; Oehr, C. *Surf. Coat. Technol.* **2001**, *142−144*, 849−855.
(54) Hegemann, D. *Thin Solid Films* **2006**, *515*, 2173−2178.
(55) Wu, Q.; Gleason, K. K. *Plasmas Polym.* **2003**, *8*, 31−41.
(56) Coopes, I. H.; Griesser, H. J. *J. Appl. Polym. Sci.* **1989**, *37*, 3413−3422.